GAMMA RAY OBSERVATIONS OF THE INTERSTELLAR CLOUDS IN CEPHEUS

NASA Grant NAG5-2823

Annual Report No. 2
for the Period 15 December 1996 through 14 December 1997

Principal Investigator
Professor Patrick Thaddeus

October 14, 1997

Prepared for

National Aeronautics and Space Administration
Washington, DC 20546

SMITHSONIAN INSTITUTION
ASTROPHYSICAL OBSERVATORY
CAMBRIDGE, MASSACHUSETTS 02138

Director: Irwin I. Shapiro

The Smithsonian Astrophysical Observatory
is a member of the
Harvard-Smithsonian Center for Astrophysics

NASA Grant NAG5-2823: "Gamma-Ray Observations of the Interstellar Clouds in Cepheus"

Report for the Period 15 December 1996 – 14 December 1997

1. Introduction

The focus of the work during this period was the analysis of the diffuse gamma-ray emission from Monoceros. The steps of the analysis completed and the results obtained are summarized below. Part of the work was presented at the 4th Compton Observatory Symposium, April 27–30 (Digel et al. 1997); a journal article is in preparation.

2. Summary of Analysis

The diffuse gamma-ray emission in Monoceros was studied in a way complementary to analyses applied to other regions, like Cepheus (Digel et al. 1996), Orion (Digel et al. 1995), and Ophiuchus (Hunter et al. 1994). The Monoceros region is very well suited for determination of the cosmic-ray density and molecular mass calibration in the outer Galaxy, i.e., beyond the solar circle.

Cosmic rays are assumed to be smoothly distributed on kiloparsec scales and the 21-cm line of H I and the 2.6-mm line of CO are assumed to trace the interstellar gas. High-energy gamma rays are produced in collisions of cosmic-ray protons and electrons with nuclei in interstellar gas. The contribution from inverse Compton scattering of photons by cosmic rays is neglected, but general isotropic gamma-ray emission is included in a model of the gamma-ray intensities observed by EGRET. The free parameters in the model, other than the isotropic intensity, are the gamma-ray emissivities and the $N(H_2)/W_{CO}$ ratio on various line-of-sight distance ranges. Other than the $N(H_2)/W_{CO}$ ratio, these parameters depend on energy. For each energy range studied, the residuals between the observed diffuse emission and the model are searched for evidence of gamma-ray point sources or possible small-scale enhancements in the cosmic-ray density.

2.1 Data Sets

The primary gamma-ray data set was compiled from all of the EGRET viewing periods that overlap any part of the region of interest ($l = 210–250°$, $b = -15 - +20°$). This included viewing periods 510 and 510.5, which were pointed observations of the central part of this field awarded specifically for this study. Owing to the proximity of the Crab and Vela pulsars to edges of the field, a very large number of viewing periods (more than 50) have at least a partial contribution to the overall EGRET exposure in the field. In order to combine all of these viewing periods, and to make consistency checks of their relative calibrations, special software was written. (The sensitivity of EGRET depends on time, and the overall exposure correction factors must be checked in this way.) For the representative energy range $E > 100$ MeV, the final gamma-ray dataset includes 19,814 photons.

The CO spectral line data for the region of interest were taken from the composite survey of the Milky Way by Dame et al. (1987) and H I spectra for the region were compiled by

combining parts of the surveys of Cleary et al. (1979), Heiles & Habing (1974), Kerr et al. (1986) and Weaver & Williams (1973). Spectral line data were actually required for an area much larger than the region of interest in Monoceros; coverage of a 15° border was included to permit the data for the central region to be convolved with the effective point spread function of EGRET, which is quite broad at the lower energies. CO data for $|b| > 5$–$10°$ are not generally available; for regions without CO observations, the reasonable assumption that no molecular gas is present was made. The relative intensity calibrations of the H I surveys were checked as part of the process of combining the surveys.

In order to study the the gamma-ray emissivity of the interstellar gas, which is proportional to the density of cosmic rays, at different distances in the outer Galaxy, maps of $N(\text{H I})$ and W_{CO} were derived for four distance ranges along the line of sight. Distances were derived kinematically in the usual way, on the assumption of a flat rotation curve across the outer Galaxy. The four distance ranges may be denoted local (Monoceros), interarm, Perseus arm, and beyond Perseus arm. No significant CO emission is detected in the Dame et al. (1987) survey in the outer two distance ranges.

2.2 The Model and Model Fitting

The model of the observed map of gamma-ray photons, i.e., the intensity map multiplied by the EGRET exposure map, is a simple linear combination of the $N(\text{H I})$ and W_{CO} maps discussed above, with a constant-intensity term corresponding to the isotropic emission. The coefficients of the linear combination, which are determined by fitting the model to the gamma-ray observations, have direct interpretations in terms of the gamma-ray emissivity and the $N(\text{H}_2)/W_{CO}$ ratio. By fitting the model to the observations for a range of energies, the emissivity spectrum can be derived, which in principle permits the cosmic-ray proton and electron components to be independently determined. In addition to the terms describing the diffuse emission, the model also required three point sources, corresponding to cataloged EGRET sources (Thompson et al. 1996).

The model was fit to the gamma-ray data set for several energy ranges spanning the 30 MeV – 10 GeV range of sensitivity of EGRET. Details of the fitting method, known as the maximum likelihood method, are given in Digel et al. (1996) along with citations to the original work on likelihood analysis in astronomy.

3. Results

Quantitative results for Monoceros are presented in the enclosed copy of Digel et al. (1997). Briefly, no evidence was seen for point sources other than those already cataloged in Thompson et al. (1996), or for localized regions of enhanced gamma-ray emissivity. The local gamma-ray emissivity was found to be consistent with previous work on different interstellar clouds. The local $N(\text{H}_2)/W_{CO}$ ratio in Monoceros was found to be somewhat larger than in closer interstellar clouds, but consistent with the general trend for larger ratios in the outer Galaxy seen in other work. Possibly the most notable finding was that the gamma-ray emissivity does not decline monotonically from the solar circle, but instead has a secondary maximum in the Perseus arm. This finding appears to support models of cosmic ray propagation in the Galaxy that predict the cosmic-ray density to be proportional to the surface density of gas on large

scales. Together with other work (Digel et al. 1996), it also suggests that the cosmic-ray density cannot be assumed to be a simple function of Galactocentric distance; instead, the density has significant azimuthal dependence, which is likely related to the spiral structure of the Milky Way.

4. Planned work through the end of the grant period

Enough analysis has been completed to warrant the preparation of a journal article describing the results for Monoceros. Some aspects of the analysis may be refined somewhat, such as a determination of quantitative limits on the variation of the gamma-ray emissivity within the local clouds in this region. The interpretation of the break in emissivity at low energies for the gas traced by CO, which may indicate cosmic-ray exclusion from molecular clouds, also needs to be considered carefully.

Many of the same analysis techniques, and many of the same data sets, may be applied to the other planned study, that of the diffuse emission toward the tangents of the spiral arms in the inner Galaxy, which will be undertaken next. This analysis will be simpler in that the regions to be studied will be smaller and contained in many fewer EGRET viewing periods. The numbers of gamma-ray photons in the data sets will be about as great as for Monoceros, however, owing to the good EGRET exposures and the relative brightness of the diffuse emission toward the inner Galaxy.

References

Cleary, M. N., Haslam, C. G. T., & Heiles, C. 1979, A&AS, 36, 95

Dame, T. M., et al. 1987, ApJ, 322, 706

Digel, S. W., Hunter, S. D., & Mukherjee, R. 1995, ApJ, 441, 270

Digel, S. W., et al. 1996, ApJ, 463, 609

Heiles, C., & Habing, H. J. 1974, A&AS, 14, 1

Hunter, S. D., et al. 1994, ApJ, 436, 216

Kerr, F. J., et al. 1986, A&AS, 66, 373

Thompson, D. J., et al. 1996, ApJS, 107, 227

Weaver, H., & Williams, D. R. W. 1973, A&AS, 8, 1

Publications resulting from this work during the reporting period

Digel, S. W., Grenier, I. A., Hunter, S. D., Dame, T. M., & Thaddeus, P. 1997, "Diffuse High-Energy Gamma-Ray Emission in Monoceros", in Proc. 4th Compton Observatory Symposium, ed. C. Dermer (AIP: New York), in press.

Diffuse High-Energy Gamma-Ray Emission in Monoceros

S. W. Digel[*], I. A. Grenier[+], S. D. Hunter[†],
T. M. Dame[**], and P. Thaddeus[**]

[*]Hughes STX, NASA/GSFC, Code 631
Greenbelt, MD 20771
[+]Université Paris 7 and Service d'Astrophysique, CE Saclay
[†]NASA/GSFC, Code 661
[**]Harvard-Smithsonian Center for Astrophysics

Abstract. We present a study of the diffuse gamma-ray emission observed by EGRET toward Monoceros in the outer Galaxy. The region studied, $l = 210 - 250°$, $b = -15 - +20°$, includes the molecular clouds associated with Mon R2 and Maddalena's cloud as well as more distant clouds in the Perseus arm. This is the sector of the third quadrant best suited for study of variations of the gamma-ray emissivity and molecular cloud mass calibration in the outer Galaxy. The molecular mass calibrating ratio in Monoceros is found to be $N(H_2)/W_{CO} = (1.56 \pm 0.29) \times 10^{20}$ cm^{-2} (K km s^{-1})$^{-1}$ and the integral gamma-ray emissivity is $Q(E > 100 \text{ MeV}) = (1.92 \pm 0.14) \times 10^{-26}$ H-atom^{-1} s^{-1} sr^{-1}. The emissivity profile across the outer Galaxy is found to have a minimum between the local interstellar clouds and those in the Perseus arm.

INTRODUCTION

The advances provided by EGRET for the detection of diffuse, high-energy gamma-ray emission have made it possible to study the spatial and spectral variation of the emission with unprecedented detail. The object of such studies, aside from identifying point sources that would otherwise be confused with diffuse emission, has been to measure the high-energy cosmic-ray proton and electron densities at remote locations, and to calibrate the CO $J = 1 \rightarrow 0$ line as a tracer of interstellar molecular hydrogen.

A number of individual interstellar cloud complexes are resolved by EGRET and have been studied in the way described here (e.g., Ophiuchus [1], Orion [2], and Cepheus [3]). The local cloud complex in Cepheus is in the foreground of distant, massive clouds in the Perseus arm. In the Galactic longitude range of Cepheus, $l \sim 100 - 130°$, the Doppler shifts of the H I and CO emission lines

from the interstellar medium are a strong function of Galactocentric distance. This consideration, and the good sensitivity of EGRET, permitted the local and distant components of the diffuse emission to be studied separately across the outer Galaxy. The approximate analog of the Cepheus region in the third quadrant is the complex of local interstellar clouds in Monoceros, which again lie in front of more distant clouds in the Perseus arm.

We undertook a study of the diffuse emission in Monoceros to compare the radial variations of cosmic-ray density and gas mass calibration in the third quadrant with that inferred in the second quadrant from the Cepheus study. Some results from this work [4] are presented here.

DATA

The gamma-ray dataset includes all relevant EGRET viewing periods through 510.0 and 510.5, which were pointed observations of Monoceros with EGRET in restricted field of view mode. Owing to the large field of view of EGRET and the proximity of the well-observed Geminga and Vela pulsars to either longitude extreme of the region of interest, more than 50 viewing periods are combined here. The intensities of the viewing periods were intercompared to check the relative calibrations. The total number of photons in the region of interest ($l = 210 - 250°$, $b = -15 - +20°$) is 19,814 for the representative energy range $E > 100$ MeV.

As tracers of the neutral interstellar gas, we use the 21-cm H I surveys of Weaver & Williams [5], Heiles & Habing [6], Cleary et al. [7], and Kerr et al. [8] and the 2.6-mm CO survey of Dame et al. [9]. For purposes of the analysis, integrated maps were constructed for four adjacent ranges of Galactocentric distance R across the outer Galaxy: 1. Monoceros local ($R < 10$ kpc); 2. Interarm ($R = 10 - 12.5$ kpc); 3. Perseus arm ($R = 12.5 - 16$ kpc); 4. Beyond Perseus arm ($R > 16$ kpc). Galactocentric distances were derived on the assumption of a flat rotation curve with $R_\odot = 8.5$ kpc and $V_\odot = 220$ km s^{-1}.

ANALYSIS

As is commonly done [1–3], we assume that the interstellar medium is transparent to high-energy gamma-rays, that the cosmic rays responsible for the gamma-ray production are uniform within each annulus and within the atomic and molecular gas, and that the $N(H_2)/W_{CO}$ proportionality (X) is constant within each annulus. Under these assumptions the observed gamma-ray intensity for a given energy range may be modeled as a linear combination of the $N(HI)$ and W_{CO} maps. Additional terms for the isotropic intensity and for four unidentified point sources in the field [10,11] must also be included; the column density of ionized hydrogen and the inverse Compton intensity

are neglected here. The CO emission in the outer two annuli was not significant and not included in the model; for any given gamma-ray energy range, the final model thus had 11 free parameters. Coefficients of the linear combination, which are directly related to the gamma-ray emissivities and the X-ratios in the annuli, are determined from a maximum likelihood fit [12,13] to the EGRET observations.
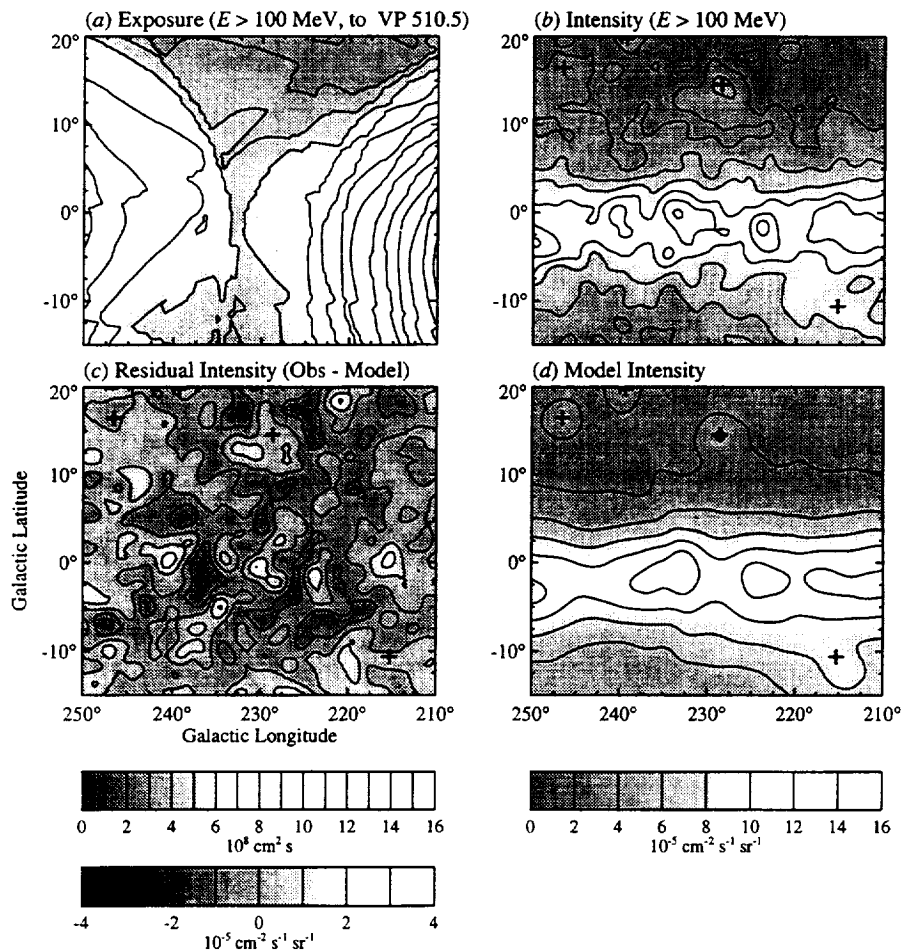

FIGURE 1. Observed and model intensities for $E > 100$ MeV. (a) The effective EGRET exposure, derived on the assumption of a gamma-ray spectral index of -2.1, is largest near the Geminga and Vela pulsars, outside the high and low longitude ranges of the region of interest. (b) Observed intensity, smoothed slightly to decrease fluctuations. The crosses mark the positions of the four point sources – all cataloged unidentified EGRET point sources [10,11] – in the model. (c) The residual intensity (observed minus model) shows no large-scale deviations from zero. (d) Model intensity, displayed with the same smoothing and contour levels as (b).

RESULTS

The model was fit to the EGRET observations for several gamma-ray energy ranges spanning 30-10,000 MeV. The observed and model gamma-ray intensities are compared in Figure 1 for $E > 100$ MeV. The residual map (Fig. 1c) has no positive fluctuations consistent with significant point sources, and has no apparent large-scale trends.

The integral gamma-ray emissivities for $E > 100$ MeV are compared in Figure 2 with the emissivities found in other large-area studies. In this energy range, the emissivity is approximately proportional to the density of high-energy cosmic-ray protons. Also shown in the figure is the profile of cosmic-ray density from the model of Hunter et al. [14] for the same longitude range, normalized at the Solar circle. The emissivity gradient in Monoceros, as the model of Hunter et al. predicts, is not monotonic with R. Rather, the emissivity has a minimum between the Solar circle and the Perseus arm. This variation may not be evident in the Strong et al. [15] and Strong & Mattox [16] emissivities, because they are averaged over essentially the entire outer Galaxy, which would tend to smear away such contrasts. The emissivity gradient found for the Cepheus longitude range [3], which would not be subject to such smearing, nevertheless does appear to be monotonic. This may be an effect of the different binning used – the Perseus arm is closer at lower longitudes and no 'Interarm' range of interstellar gas could be defined. Another possible interpretation is that the 1.8 kpc scale length for gas-cosmic ray
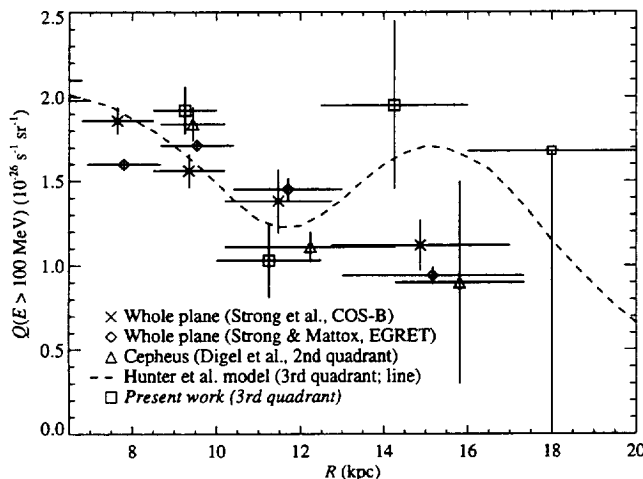

FIGURE 2. The derived emissivity gradient toward Monoceros for $E > 100$ MeV; one point is plotted for each annulus. For comparison, also shown are the profile of cosmic-ray enhancement for the third quadrant from the model of Hunter et al. [14], the gradient derived from an EGRET study of the Cepheus region in the second quadrant [3], and the whole-Galaxy averages of Strong et al. [15] and Strong & Mattox [16].

coupling in the model of Hunter et al. [14] spans the interarm gap in Cepheus but not the broader gap ($\sim$2.5 kpc) in Monoceros.

The X-ratio for the local annulus, the principal molecular clouds of which are Mon R2 and CMa OB1, is $N(H_2)/W_{CO} = (1.56 \pm 0.29) \times 10^{20}$ cm^{-2} (K km s^{-1})$^{-1}$. This is somewhat greater than found for other, closer, molecular clouds in recent studies, e.g., Ophiuchus 1.1 ± 0.2 [1], Orion 1.06 ± 0.14 [2], and Cepheus 0.92 ± 0.14 [3] in the same units. However, the clouds in Monoceros have Galactocentric distance several hundred parsecs greater than these others; the magnitude of the difference of X is consistent with a generally increasing trend found beyond the solar circle, which may be related to overall gradients of cloud temperature or abundances (e.g., [17–19]).

CONCLUSIONS

Our study of diffuse gamma-ray emission in Monoceros indicates that the density profile of high-energy protons may have a secondary maximum in the Perseus arm, where the cosmic-ray density is approximately the same as it is in the Solar vicinity. The X-ratio for the clouds in Monoceros is somewhat larger than for other local clouds, but they are significantly more distant, in the direction where there is already evidence that the ratio tends to increase.

REFERENCES

1. Hunter, S. D., et al., *ApJ* **436**, 216 (1994)
2. Digel, S. W., Hunter, S. D., & Mukherjee, R., *ApJ* **441**, 270 (1995).
3. Digel, S. W., et al., *ApJ* **463**, 609 (1996).
4. Digel, S. W., et al., *ApJ* in prep.
5. Weaver, H., & Williams, D. R. W., *A&AS* **8**, 1 (1973).
6. Heiles, C., & Habing, H. J., *A&AS* **14**, 1 (1974).
7. Cleary, M. N., Haslam, C. G. T., & Heiles, C., *A&AS* **36**, 95 (1979).
8. Kerr, F. J., et al., *A&AS* **66**, 373 (1986).
9. Dame, T. M., et al., *ApJ* **322**, 706 (1987).
10. Fichtel, C. E., et al., *ApJS* **94**, 551 (1994).
11. Thompson, D. J., et al., *ApJS* **107**, 227 (1996).
12. Pollock, A. M. T., et al., *A&A* **146**, 352 (1985).
13. Mattox, J. R., et al., *ApJ* **461**, 396 (1996).
14. Hunter, S. D. et al., *ApJ* **481**, 205 (1997).
15. Strong, A., et al., *A&A* **207**, 1 (1988).
16. Strong, A. & Mattox, J. R., *A&A* **308**, 21L (1996).
17. Mead, K. N., & Kutner, M. L., *ApJ* **330**, 399 (1988).
18. Digel, S., Bally, J., & Thaddeus, P., *ApJ* **357**, L29 (1990).
19. Sodroski, T. J., *ApJ* **366**, 95 (1991).